

Quantum squeezing induced quantum entanglement and EPR steering in coupled optomechanical system

SHAO-XIONG WU,^{1,2,*}, CHENG-HUA BAI,¹ GANG LI,^{2,3} CHANG-SHUI YU,^{4,†} AND TIANCAI ZHANG^{2,3,‡}

¹ School of Semiconductor and Physics, North University of China, Taiyuan 030051, China

² State Key Laboratory of Quantum Optics and Quantum Optics Devices, and Institute of Opto-Electronics, Shanxi University, Taiyuan 030006, China

³ Collaborative Innovation Center of Extreme Optics, Shanxi University, Taiyuan 030006, China

⁴ School of Physics, Dalian University of Technology, Dalian 116024, China

*sxwu@nuc.edu.cn

†yys@dlut.edu.cn

‡tczhang@sxu.edu.cn

Abstract: We propose a theoretical project in which quantum squeezing induces quantum entanglement and Einstein-Podolsky-Rosen steering in a coupled whispering-gallery-mode optomechanical system. Through pumping the $\chi^{(2)}$ -nonlinear resonator with the phase matching condition, the generated squeezed resonator mode and the mechanical mode of the optomechanical resonator can generate strong quantum entanglement and EPR steering, where the squeezing of the nonlinear resonator plays the vital role. The transitions from zero entanglement to strong entanglement and one-way steering to two-way steering can be realized by adjusting the system parameters appropriately. The photon-photon entanglement and steering between the two resonators can also be obtained by deducing the amplitude of the driving laser. Our project does not need an extraordinarily squeezed field, and it is convenient to manipulate and provides a novel and flexible avenue for diverse applications in quantum technology dependent on both optomechanical and photon-photon entanglement and steering.

© 2023 Optica Publishing Group under the terms of the [Optica Open Access Publishing Agreement](#)

1. Introduction

Quantum entanglement is not only one of the main striking features that distinguishes quantum physics from the classical world but also a fundamental resource in quantum information technology. In particular, the entanglement between microscopic and macroscopic matter is of significance to the basic theory of quantum mechanics both theoretically and experimentally. Due to the connection between microscopic matter (such as photons) and macroscopic matter (such as mechanical oscillators), the optomechanical system is a promising, flexible, and sensitive experimental platform to test and take advantage of the non-classical effects of quantum systems at the single-photon level [1]. The high quality optomechanical microcavities can be manufactured with the development of experimental technology, especially the micro/nano fabrication technique. How to realize strong and steady-state continuous entanglement is one of the essential issues in optomechanics research. After pioneering works on entanglement between a movable mirror and cavity field [2, 3], optomechanical entanglement has been widely studied theoretically and experimentally and has becoming a booming research field. Scholars have realized strong steady-state entanglement in various ways based on different systems, such as auxiliary-cavity-assisted optomechanical systems [4], generating entanglement by gently modulating optomechanical systems [5, 6], using continuous measurement and feedback control [7], nonreciprocal optomechanical entanglement in spin microresonator [8], noise-tolerant optomechanical entanglement via synthetic magnetism [9], utilizing the dual-mode cooling effect [10] or

dark resonance [11], modulating two driving fields [12], experimental demonstration by atomic ensembles [13], and tri-particle optomechanical entanglement [14–16].

As another kind of quantum non-locality, Einstein-Podolsky-Rosen (EPR) steering was proposed in the ideological experiment of the nonlocal problem between two-body systems, which denotes how to control or manipulate quantum entanglement [17–19]. In recent decades, the quantitative measurement of EPR steering has been mathematically defined [20, 21], where EPR steering is stronger than quantum entanglement but weaker than Bell nonlocality under the hierarchy of quantum nonlocality. Due to the intrinsic asymmetry, EPR steering may play a more fundamental role than quantum entanglement in nontrusted quantum communication. The properties of EPR steering and its applications [22–28] in quantum technology have been widely reported. In optomechanical systems, EPR steering has also attracted attention, such as asymmetric EPR steering via a single dissipation pathway [29], enhancing EPR steering between two mechanical modes [30], manipulating asymmetric steering via interference effects [31], and EPR steering between distant macroscopic systems [32]. At the same time, the realization of quantum entanglement or EPR steering is often accompanied by squeezing or cooling of the mechanical mode, and realization squeezing beyond 3dB or ground state cooling of the mechanical oscillator have also been extensively reported [33–43].

The squeezed state is a valuable resource in quantum optics and has many applications in various quantum processes. Under the phase matching conditions, the spontaneous parametric down conversion process can occur by employing $\chi^{(2)}$ -nonlinear matter, and a squeezed process can be realized in the Bogoliubov transformation picture without an external squeezed field. In an optomechanical system, the nonlinear interaction between the squeezed cavity mode and mechanical mode can lead to a strong single-photon interaction [44]. A similar mechanism can be used to enhance the atom-field cooperativity parameter [45], strengthen the coherent dipole coupling between two atoms [46], explore the quantum speed limit in the squeezed optical cavity mode [47], and realize optical nonreciprocity induced by squeezing in a whispering-gallery-mode (WGM) cavity [48]. As a kind of common optical cavity, the WGM cavity has been applied to demonstrate the non-Hermitian physics [49, 50], the optomechanically-induced transparency phenomenon [51], the phase-controlled nonreciprocal routing [52], the phonon laser enhancement via optomechanics interaction [53], the nonreciprocal photon blockade in squeezed mode [54], and the effect of optomechanical entanglement by exceptional point [55].

Inspired and encouraged by the above works, we systematically investigate the quantum entanglement and EPR steering induced by quantum squeezing in a coupled WGM optomechanical system in this paper. First, we focus on the entanglement and steering between the mechanical mode and the indirect interacted optical mode. Strong steady-state entanglement and steering can be achieved by properly optimizing the squeezing parameter, where the squeezing of the $\chi^{(2)}$ -nonlinear resonator plays the central role in the generating quantum nonlocality. Second, we consider the photon-photon entanglement and steering between the coupled resonators by changing the amplitude of the driving laser. Unlike the quantum entanglement and EPR steering in cavity magnomechanical system via a squeezed vacuum field, the enhancement of quantum entanglement and EPR steering does not need an external squeezed field [56, 57] or the method of reservoir engineering [58, 59].

The structure of this paper is as follows. In Sec. 2, we introduce the model of this project and derive the effective Hamiltonian by utilizing the quantum Langevin equation. In Sec. 3, we investigate the entanglement and steering between the $\chi^{(2)}$ -nonlinear resonator and the mechanical oscillator, where the squeezing parameter plays an indispensable role in the generation of strong steady-state entanglement and steering, and discuss how to realize the transition from zero entanglement to strong entanglement and one-way steering to two-way steering. In Sec. 4, we study the entanglement and steering between the two resonator and show the transformation between steerable modes by changing the decay rate of resonators.

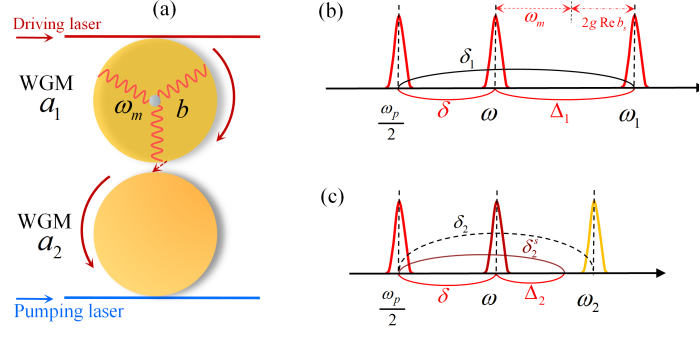


Fig. 1. (a) Sketched diagrams of the project. It consists of two coupled WGM resonators: the optomechanical resonator is driven by a coherent laser, and a $\chi^{(2)}$ -nonlinear resonator is pumped under phase matching conditions. (b) The frequency relationship of resonator a_1 . (c) The frequency relationship of resonator a_2 . In the squeezing picture, a symbol s is marked in the superscript.

2. The model and linearized effective Hamiltonian

The coupled WGM optomechanical system model is depicted in Fig. 1(a). The Hamiltonian (in units of \hbar) of the whole system can be given as

$$\begin{aligned}
 H_0 = & \omega_1 a_1^\dagger a_1 + \omega_2 a_2^\dagger a_2 + \omega_m b^\dagger b - g a_1^\dagger a_1 (b + b^\dagger) + J(a_1^\dagger a_2 + a_1 a_2^\dagger) \\
 & + iE(a_1^\dagger e^{-i\omega t} - a_1 e^{i\omega t}) + \frac{\Omega_p}{2}(e^{-i\theta} a_2^{\dagger 2} e^{-i\omega_p t} + e^{i\theta} a_2^2 e^{i\omega_p t}), \quad (1)
 \end{aligned}$$

where a_i and ω_i ($i = 1, 2$) express the annihilation operator and frequency of the i -th resonator's optical mode, and b and ω_m denote the annihilation operator and frequency of the mechanical mode. The optomechanical resonator a_1 is driven by a coherent laser with amplitude E and frequency ω , and the single-photon coupling strength between the mechanical mode b and optical mode a_1 is g . The coupling strength between the two optical resonators is J . The resonator a_2 is made up of high-quality materials with $\chi^{(2)}$ nonlinearity, e.g., lithium niobate or aluminum nitride [48, 51], and pumped by a coherent laser with frequency ω_p , which can generate squeezing interaction with strength Ω_p under phase-matching conditions through the parametric down-conversion process. Due to the different kinds of materials, detuning or phase matching conditions between resonators a_1 and a_2 , the cavity mode of resonator a_1 is not squeezed.

In the frame rotating under frequency $\omega_p/2$, i.e., $U_0^\dagger H_0 U_0 - iU_0^\dagger \dot{U}_0$ with $U_0 = \exp[-i\frac{\omega_p}{2}t(a_1^\dagger a_1 + a_2^\dagger a_2)]$, the system Hamiltonian (1) can be rewritten as

$$\begin{aligned}
 H_r = & \delta_1 a_1^\dagger a_1 + \delta_2 a_2^\dagger a_2 + \omega_m b^\dagger b - g a_1^\dagger a_1 (b + b^\dagger) + J(a_1^\dagger a_2 + a_1 a_2^\dagger) \\
 & + iE(a_1^\dagger e^{-i\delta t} - a_1 e^{i\delta t}) + \frac{\Omega_p}{2}(e^{-i\theta} a_2^{\dagger 2} + e^{i\theta} a_2^2), \quad (2)
 \end{aligned}$$

where the detuning parameters are $\delta_1 = \omega_1 - \omega_p/2$, $\delta_2 = \omega_2 - \omega_p/2$, and $\delta = \omega - \omega_p/2$. Resonator a_2 can be transformed to the squeezing picture by applying the Bogoliubov transformation $a_2^s = S(r)a_2 S^\dagger(r) = \cosh r a_2 + e^{-i\theta} \sinh r a_2^\dagger$, where $S(r) = \exp[r e^{i\theta} (a_2^2 - a_2^{\dagger 2})]$ is the single-mode squeezing operator and $r = \frac{1}{2} \operatorname{arctanh} \beta$ is the squeezing parameter with a tunable coefficient $\beta = \Omega_p / \delta_2$. According to the inverse hyperbolic tangent function's domain, the amplitude Ω_p value should be smaller than the detuning of resonator a_2 . In the squeezing picture, the rotating-wave approximation (RWA) can be employed under the weak coupling condition, i.e.

$\delta_1 + \delta_2^s \gg \sinh rJ$, and Hamiltonian (2) can be simplified as

$$H_{\text{rwa}} = \delta_1 a_1^\dagger a_1 + \delta_2^s a_2^{s\dagger} a_2^s + \omega_m b^\dagger b - g a_1^\dagger a_1 (b + b^\dagger) + J^s (a_1^\dagger a_2^s + a_1 a_2^{s\dagger}) + iE (a_1^\dagger e^{-i\delta t} - a_1 e^{i\delta t}), \quad (3)$$

where $\delta_2^s = \delta_2 \sqrt{1 - \beta^2}$ is the detuning of resonator a_2 in the squeezing picture, and $J^s = \cosh rJ$ is the effective coupling strength between the two resonators.

Continuing to apply frame rotation with detuning δ , Hamiltonian (3) can be described by

$$H = \Delta_1 a_1^\dagger a_1 + \Delta_2 a_2^{s\dagger} a_2^s + \omega_m b^\dagger b - g a_1^\dagger a_1 (b + b^\dagger) + J^s (a_1^\dagger a_2^s + a_1 a_2^{s\dagger}) + iE (a_1^\dagger - a_1) \quad (4)$$

with the detuning parameters $\Delta_1 = \delta_1 - \delta$ and $\Delta_2 = \delta_2^s - \delta$. The frequency relationship between the driving and pumping lasers and the resonators is shown vividly in Fig. 1(b) and (c). For simplicity and without loss of generality, the red detuning between the resonator a_1 and the driving laser, i.e., $\Delta_1 = \omega_1 - \omega$, is assumed to match the sum of the mechanical oscillator frequency ω_m and the displacement of detuning $2g\text{Re}b_s$ (see Eq. (7)) induced by the optomechanical interaction. In the following, we will investigate the dynamical behavior of the whole optomechanical system, and the symbol a_2^s will be shorted as a_2 without ambiguity. In Fig. 1(c), δ_2 expresses the detuning between the resonator a_2 and the pumping laser without the squeezing picture, expressed by the black dashed line. In contrast, the corresponding detuning in the squeezing picture is δ_2^s , denoted by the crimson line.

Taking into account the dissipation and the corresponding environmental noise of the resonators a_1 , a_2 and the mechanical oscillator b , the dynamics of the optomechanical system can be described by the nonlinear quantum Langevin equations [60, 61]:

$$\begin{aligned} \dot{a}_1 &= (-i\Delta_1 - \frac{\kappa_1}{2})a_1 - iJ^s a_2 + ig a_1 (b + b^\dagger) + E + \sqrt{\kappa_1} a_1^{\text{in}}, \\ \dot{a}_2 &= (-i\Delta_2 - \frac{\kappa_2}{2})a_2 - iJ^s a_1 + \sqrt{\kappa_2} a_2^{\text{in}}, \\ \dot{b} &= (-i\omega_m - \frac{\gamma_m}{2})b + ig a_1^\dagger a_1 + \sqrt{\gamma_m} b^{\text{in}}, \end{aligned} \quad (5)$$

where κ_i and γ_m are the decay rates of resonator a_i and the mechanical oscillator, respectively, and a_i^{in} and b^{in} are the corresponding zero-mean environment noise operators. Notice that the decay rate κ_2 will not be changed in the squeezing picture.

The quantum Langevin equations in Eq. (5) can be solved by the standard linearization process under a strong external coherent driving laser, and the operators of resonator a_i and mechanical oscillator b can be rewritten as the sum of steady-state mean values and quantum fluctuation operators, i.e., $o = o_s + \delta o$ ($o = a_i, b$). The differential equations for the steady-state mean values are

$$\begin{aligned} \dot{a}_{1s} &= (-i\Delta_1' - \frac{\kappa_1}{2})a_{1s} - iJ^s a_{2s} + E, \\ \dot{a}_{2s} &= (-i\Delta_2 - \frac{\kappa_2}{2})a_{2s} - iJ^s a_{1s}, \\ \dot{b}_s &= (-i\omega_m - \frac{\gamma_m}{2})b_s + ig |a_{1s}|^2, \end{aligned} \quad (6)$$

where the effective detuning $\Delta_1' = \Delta_1 - 2g\text{Re}b_s$. For the steady state, its operator mean value is not changed with time, and Eq. (6) can be solved as

$$a_{1s} = \frac{E(i\Delta_2 + \frac{\kappa_2}{2})}{J^s + (i\Delta_1' + \frac{\kappa_1}{2})(i\Delta_2 + \frac{\kappa_2}{2})}, \quad b_s = \frac{ig |a_{1s}|^2}{i\omega_m + \frac{\gamma_m}{2}}. \quad (7)$$

By adjusting the phase of the driving laser, the value of a_{1s} can be considered as a real number, and the following form determines the linearized quantum Langevin equations for the quantum fluctuation operators:

$$\begin{aligned}\delta\dot{a}_1 &= (-i\Delta'_1 - \frac{\kappa_1}{2})\delta a_1 - iJ^s \delta a_2 + i g a_{1s}(\delta b + \delta b^\dagger) + \sqrt{\kappa_1} a_1^{\text{in}}, \\ \delta\dot{a}_2 &= (-i\Delta_2 - \frac{\kappa_2}{2})\delta a_2 - iJ^s \delta a_1 + \sqrt{\kappa_2} a_2^{\text{in}}, \\ \delta\dot{b} &= (-i\omega_m - \frac{\gamma_m}{2})\delta b + i g a_{1s}(\delta a_1 + \delta a_1^\dagger) + \sqrt{\gamma_m} b^{\text{in}}.\end{aligned}\quad (8)$$

According to Eq. (8), the effective Hamiltonian of quantum fluctuation operators can be obtained as

$$\begin{aligned}H_{\text{eff}} &= \Delta'_1 \delta a_1^\dagger \delta a_1 + \Delta_2 \delta a_2^\dagger \delta a_2 + J^s (\delta a_1 \delta a_2^\dagger + \delta a_1^\dagger \delta a_2) \\ &+ \omega_m \delta b^\dagger \delta b - G (\delta a_1 + \delta a_1^\dagger) (\delta b^\dagger + \delta b)\end{aligned}\quad (9)$$

with the effective optomechanical coupling strength $G = g a_{1s}$. For the weak coupling regime and employing the RWA approximation, the effective linearized Hamiltonian arrives at

$$\begin{aligned}H_{\text{lin}} &= \Delta'_1 \delta a_1^\dagger \delta a_1 + \Delta_2 \delta a_2^\dagger \delta a_2 + J^s (\delta a_1 \delta a_2^\dagger + \delta a_1^\dagger \delta a_2) \\ &+ \omega_m \delta b^\dagger \delta b - G (\delta a_1 \delta b^\dagger + \delta a_1^\dagger \delta b).\end{aligned}\quad (10)$$

The coefficients in Hamiltonian (10), i.e., the effective detuning Δ'_1 , Δ_2 , the effective coupling strength J^s , and the effective optomechanical coupling strength G , are affected by the squeezing of the resonator a_2 . For simplicity and without loss of generality, the value of the effective detuning Δ'_1 is assumed to be the same as that of ω_m in what follows.

Because of the squeezing transformation of the resonator a_2 , the nonzero noise correlation functions of operator a_2^{in} will be turned into the squeezing picture and read $\langle a_2^{\text{in}\dagger}(t) a_2^{\text{in}}(\tau) \rangle = N \delta(t-\tau)$, $\langle a_2^{\text{in}}(t) a_2^{\text{in}\dagger}(\tau) \rangle = (N+1) \delta(t-\tau)$, $\langle a_2^{\text{in}}(t) a_2^{\text{in}}(\tau) \rangle = M \delta(t-\tau)$, and $\langle a_2^{\text{in}\dagger}(t) a_2^{\text{in}\dagger}(\tau) \rangle = M^* \delta(t-\tau)$ with $N = \sinh^2 r$ and $M = \cosh r \sinh r \exp(-i\theta)$ under the Markovian approximation [60, 61]. The non-zero noise correlation functions of operators a_1^{in} and b^{in} meet: $\langle a_1^{\text{in}\dagger}(t) a_1^{\text{in}}(\tau) \rangle = 0$, $\langle a_1^{\text{in}}(t) a_1^{\text{in}\dagger}(\tau) \rangle = \delta(t-\tau)$, $\langle b^{\text{in}\dagger}(t) b^{\text{in}}(\tau) \rangle = m \delta(t-\tau)$, and $\langle b^{\text{in}}(t) b^{\text{in}\dagger}(\tau) \rangle = (m+1) \delta(t-\tau)$, where $m = [\exp(\hbar\omega_m/k_B T) - 1]^{-1}$ is the thermal mean phonon number of mechanical oscillator b with temperature T .

To investigate the dynamics of the system, we will define the position and momentum quadrature fluctuation operators and noise operators as

$$\begin{aligned}X_o &= \frac{o + o^\dagger}{\sqrt{2}}, Y_o = \frac{o - o^\dagger}{i\sqrt{2}}, \\ X_{o^{\text{in}}} &= \frac{o^{\text{in}} + o^{\text{in}\dagger}}{\sqrt{2}}, Y_{o^{\text{in}}} = \frac{o^{\text{in}} - o^{\text{in}\dagger}}{i\sqrt{2}},\end{aligned}\quad (11)$$

where the operators are $o = \delta a_1, \delta a_2, \delta b$ and $o^{\text{in}} = a_1^{\text{in}}, a_2^{\text{in}}, b^{\text{in}}$. The vector of the quadrature fluctuation operators is set as $\mathcal{R}(t) = [X_{\delta a_1}, Y_{\delta a_1}, X_{\delta a_2}, Y_{\delta a_2}, X_{\delta b}, Y_{\delta b}]^T$, and the corresponding vector of the quadrature noise operators is $\mathcal{N}(t) = [X_{a_1^{\text{in}}}, Y_{a_1^{\text{in}}}, X_{a_2^{\text{in}}}, Y_{a_2^{\text{in}}}, X_{b^{\text{in}}}, Y_{b^{\text{in}}}]^T$. Based on the linearized quantum Langevin equations (8), the dynamics of the optomechanical system can be converted to a matrix form

$$\frac{d\mathcal{R}(t)}{dt} = \mathcal{M}(t)\mathcal{R}(t) + \mathcal{N}(t),\quad (12)$$

where the drift matrix $\mathcal{M}(t)$ is a 6×6 matrix with the following form

$$\mathcal{M}(t) = \begin{bmatrix} -\frac{\kappa_1}{2} & \Delta'_1 & 0 & J^s & 0 & -G \\ -\Delta'_1 & -\frac{\kappa_1}{2} & -J^s & 0 & G & 0 \\ 0 & J^s & -\frac{\kappa_2}{2} & \Delta_2 & 0 & 0 \\ -J^s & 0 & -\Delta_2 & -\frac{\kappa_2}{2} & 0 & 0 \\ 0 & -G & 0 & 0 & -\frac{\gamma_m}{2} & \omega_m \\ G & 0 & 0 & 0 & -\omega_m & -\frac{\gamma_m}{2} \end{bmatrix}. \quad (13)$$

Since the dynamical evolution of the quadrature fluctuation operators (11) is governed by the linearized Hamiltonian H_{lin} (10), the quadrature fluctuation operators can form a three-mode Gaussian state due to the intrinsic Gaussian nature of quantum noise. The Gaussian state can be characterized by a 6×6 covariance matrix $\mathcal{V}(t)$ with component $\mathcal{V}_{kl} = \langle \mathcal{R}_k \mathcal{R}_l + \mathcal{R}_l \mathcal{R}_k \rangle / 2$, and its dynamics are determined by the motion equation:

$$\frac{d\mathcal{V}}{dt} = \mathcal{M}\mathcal{V} + \mathcal{V}\mathcal{M}^T + \mathcal{D}, \quad (14)$$

where \mathcal{D} is the noise diffusion matrix with element $\mathcal{D}_{kl} = \langle N_k N_l + N_l N_k \rangle / 2$. According to the correlation functions, the noise diffusion matrix \mathcal{D} has a direct sum form

$$\mathcal{D} = \mathcal{D}_1 \oplus \mathcal{D}_2 \oplus \mathcal{D}_3 \quad (15)$$

with subblock matrices

$$\begin{aligned} \mathcal{D}_1 &= \frac{\kappa_1}{2} \text{diag}[1, 1], \\ \mathcal{D}_2 &= \frac{\kappa_2}{2} \begin{bmatrix} 2N + 1 + M + M^* & i(M^* - M) \\ i(M^* - M) & 2N + 1 - M - M^* \end{bmatrix}, \\ \mathcal{D}_3 &= \frac{\gamma_m}{2} \text{diag}[2m + 1, 2m + 1]. \end{aligned} \quad (16)$$

The reduced two-mode state among the three-mode Gaussian state can be described by a 4×4 covariance matrix with block matrix form

$$\mathcal{V}_{12} = \begin{bmatrix} \mathcal{V}_1 & \mathcal{V}_c \\ \mathcal{V}_c^T & \mathcal{V}_2 \end{bmatrix}, \quad (17)$$

where the 2×2 subblock matrices \mathcal{V}_1 , \mathcal{V}_2 and \mathcal{V}_c correspond to the subblock covariance matrices of modes 1 and 2 and their correlated parts, respectively. The two-mode Gaussian entanglement can be measured by logarithmic Negativity [62–64]:

$$E_N = \max[0, -\ln 2\eta^-] \quad (18)$$

with the coefficients $\eta^- = \sqrt{\Sigma - \sqrt{\Sigma^2 - 4 \det \mathcal{V}_{12}} / \sqrt{2}}$ and $\Sigma = \det \mathcal{V}_1 + \det \mathcal{V}_2 - 2 \det \mathcal{V}_c$. As another nonlocality measure, the EPR steering from mode 1 to 2, i.e., mode 1 can steer mode 2, is defined [21] as

$$\mathcal{G}_{1 \rightarrow 2} = \max \left[0, \frac{1}{2} \ln \frac{\det \mathcal{V}_1}{4 \det \mathcal{V}_{12}} \right]. \quad (19)$$

Similarly, the EPR steering from mode 2 to 1 is $\mathcal{G}_{2 \rightarrow 1} = \max[0, \frac{1}{2} \ln \frac{\det \mathcal{V}_2}{4 \det \mathcal{V}_{12}}]$. In the following, we will investigate the influence of quantum squeezing of resonator a_2 on the optomechanical system's quantum entanglement and EPR steering.

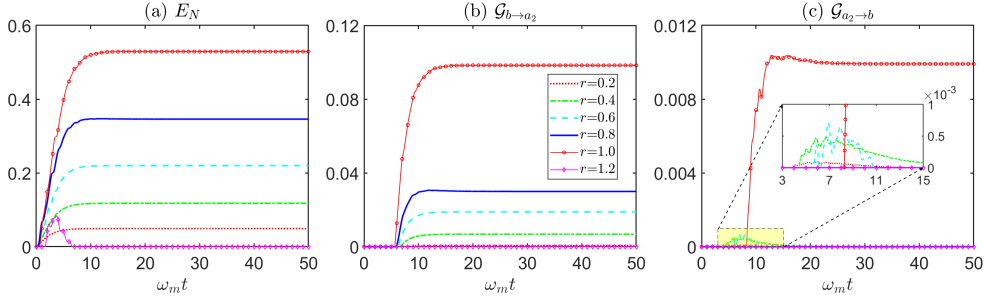


Fig. 2. The dynamics of entanglement E_N (a), steering $\mathcal{G}_{b \rightarrow a_2}$ (b), and $\mathcal{G}_{a_2 \rightarrow b}$ (c) as functions of time. The frequency of the mechanical oscillator is $\omega_m = 2\pi \times 23.4\text{MHz}$, and the other parameters are set: $\kappa_1/\omega_m = 0.6$, $\kappa_2 = \kappa_1$, $\gamma_m/\omega_m = 10^{-5}$, $J/\omega_m = 1$, $g/\omega_m = 8.5 \times 10^{-5}$, and $E/\omega_m = 3.7 \times 10^5$.

3. Entanglement and steering of resonator a_2 and mechanical oscillator b

In this section, we will first consider the optomechanical entanglement between the resonator a_2 and the mechanical oscillator b based on the effective linear Hamiltonian, which is indirectly interacted through the beam-splitter interaction among the modes $\delta a_1 - \delta b$ and $\delta a_1 - \delta a_2$. In Fig. 2, we plot the dynamics of the quantum entanglement E_N (a) and EPR steering $\mathcal{G}_{b \rightarrow a_2}$ (b), $\mathcal{G}_{a_2 \rightarrow b}$ (c) between the resonator a_2 and mechanical oscillator b under different squeezing parameters. Based on the current experimental technique, the system parameters can be chosen as: $\omega_m = 2\pi \times 23.4\text{MHz}$, $\kappa_1/\omega_m = 0.6$, $\kappa_2 = \kappa_1$, $\gamma_m/\omega_m = 10^{-5}$, $J/\omega_m = 1$, $g/\omega_m = 8.5 \times 10^{-5}$, and $E/\omega_m = 3.7 \times 10^5$. The power of the 1550nm continuous wave tunable driving laser is $P_{\text{in}} = \omega E^2/\kappa \approx 6.9\text{mW}$, and the squeezing of the resonator mode δa_2 induced by the pumping laser is essential to generate quantum nonlocality in both quantum entanglement and EPR steering. When the pumping laser is absent, i.e. $r = 0$, the entanglement and steering are zero. As the pumping strength Ω_p increases, the squeezing parameter r will be enhanced. For $r = 0.2$ (red dotted line), there exists steady entanglement; however, the steering $\mathcal{G}_{b \rightarrow a_2}$ is zero, while there is transient but unstable steering $\mathcal{G}_{a_2 \rightarrow b}$ in the dynamical evolution (shown in the inset of panel (c)). When the squeezing strength r is continued to be raised, such as $r = 0.4$ (green dotted-dashed line) or 0.6 (cyan dashed line), there is steady entanglement and steering $\mathcal{G}_{b \rightarrow a_2}$, while the behavior of the steering $\mathcal{G}_{a_2 \rightarrow b}$ is similar to that under the condition $r = 0.2$ and the steady steering $\mathcal{G}_{a_2 \rightarrow b}$ is zero. As r increases to 0.8 (blue solid line), the value of steady entanglement E_N and steering $\mathcal{G}_{b \rightarrow a_2}$ will increase with the squeezing parameter r ; however, there is no steering $\mathcal{G}_{a_2 \rightarrow b}$ in the whole dynamical evolution. When the squeezing parameter is $r = 1$ (red circle line), both the value of entanglement E_N and steering $\mathcal{G}_{b \rightarrow a_2}$ can be greatly enhanced; more importantly, steady steering $\mathcal{G}_{a_2 \rightarrow b}$ exists. However, when the squeezing parameter becomes $r = 1.2$ (magenta diamond line), there is no steady entanglement and steering. One can find that the squeezing of resonator a_2 plays a crucial role in the generating entanglement and steering between the resonator mode δa_2 and mechanical mode δb .

The physical mechanism interpretation behind the steady entanglement may be explained as follows. For the red-detuning driving, the Hamiltonian (10) can be dealt with in principle as the form $\eta(\delta a_1 \beta^\dagger + \delta a_1^\dagger \beta)$ with the Bogoliubov mode $\beta = \cosh \lambda \delta b + \sinh \lambda \delta a_2^\dagger$, where $\eta = \sqrt{G^2 - J^2}$ is the coupling strength between the resonator mode δa_1 and Bogoliubov mode β , and $\lambda = \text{arctanh}(J^2/G)$ can be considered as a squeezing coefficient of the two-mode squeezing operator $S(\lambda) = \exp[\lambda(\delta b \delta a_2 - \delta b^\dagger \delta a_2^\dagger)]$. According to the Duan-Simon criterion [65, 66], the modes δb and δa_2 of the Bogoliubov mode β are entangled, which is closely related to the squeezing coefficient λ . Due to the beam-splitter interaction, the Bogoliubov mode β can be

cooled by the resonator mode δa_1 . Intuitively, the steady entanglement between the modes δb and δa_2 is maximized when the Bogoliubov mode β is cooled to the ground state through the resonator mode δa_1 , and the squeezing coefficient λ should be as large as possible. However, the coupling strength η between the resonator mode δa_1 and Bogoliubov mode β will decrease with increasing effective coupling strength J^s between the resonators a_1 and a_2 , which will reduce the cooling effect and limit the generation of entanglement. The coefficients J^s and G are related to the squeezing parameter r induced by the pumping laser on the resonator a_2 , and strong quantum entanglement and EPR steering can be obtained by balancing the comprehensive interaction and optimizing the squeezing parameter r , which is determined by the pumping laser.

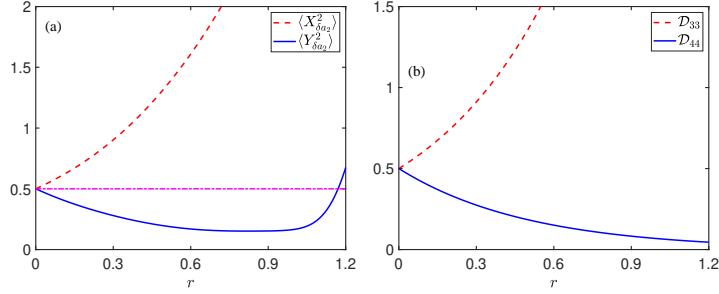


Fig. 3. (a) The variance of $\langle X_{\delta a_2} \rangle$ and $\langle Y_{\delta a_2} \rangle$ as a function of squeezing parameter r . (b) The variation (in units of κ_1) of the elements of noise matrix \mathcal{D}_{33} and \mathcal{D}_{44} along with the squeezing parameter r .

According to the generation mechanism of quantum entanglement and steering between the resonator mode δa_2 and mechanical mode δb , we plot the variation in the variances of position $\langle X_{\delta a_2}^2 \rangle$ and moment $\langle Y_{\delta a_2}^2 \rangle$ along with the squeezing parameter r in Fig. 3(a). It is easy to find that the variance of position $\langle X_{\delta a_2}^2 \rangle$ increases monotonically with increasing r . The variance of moment $\langle Y_{\delta a_2}^2 \rangle$ decreases at first, reaches a minimum value of 0.152 (corresponding to $r \approx 0.84$) and maintains a small value until $r \approx 1$. Then, the value of $\langle Y_{\delta a_2}^2 \rangle$ grows and returns back to 0.5 for $r \approx 1.18$, and the moment operator cannot be squeezed. One can also check that there is no squeezing of the position and the moment operator for the resonator mode δa_1 and mechanical mode δb . The generation of entanglement is accompanied by the occurrence of squeezing, so the moment operator squeezing of the resonator mode δa_2 induces entanglement with the mechanical mode δb through the resonator mode δa_1 as an intermediate interaction. The squeezing is the necessary condition for generating entanglement in this project. The strength of entanglement is strongly related to the squeezing parameter r . To analyze the reason why the moment operator of mode δa_2 can be squeezed, we plot the dynamics of the elements of the noise subblock diffusion matrix \mathcal{D}_{33} and \mathcal{D}_{44} in Fig. 3(b). Under a constant phase, for example, $\theta = 0$, the behavior of \mathcal{D}_{33} and \mathcal{D}_{44} exhibit opposite tendencies with increasing r , and \mathcal{D}_{33} acts like a heating bath, which will lead the variance of position $\langle X_{\delta a_2}^2 \rangle$ to continue to increase, while \mathcal{D}_{44} acts like a cooling bath and makes the value of $\langle Y_{\delta a_2}^2 \rangle$ decrease. However, the variance of moment $\langle Y_{\delta a_2}^2 \rangle$ is also influenced by \mathcal{D}_{33} and shows behavior that decrease first and then increases as r increases under the two opposite competing comprehensive effects, and the squeezing of the noise matrix is transferred to the mode δa_2 , which contributes to the entanglement between the modes δa_2 and δb .

Since steady correlation is essential in quantum technology, we will focus on steady entanglement and steering in the following content. According to the above analysis, quantum entanglement and EPR steering can be generated and enhanced with adequate squeezing parameter r . In Fig. 4, we plot the variation of entanglement E_N and steering $\mathcal{G}_{b \rightarrow a_2}$ and $\mathcal{G}_{a_2 \rightarrow b}$

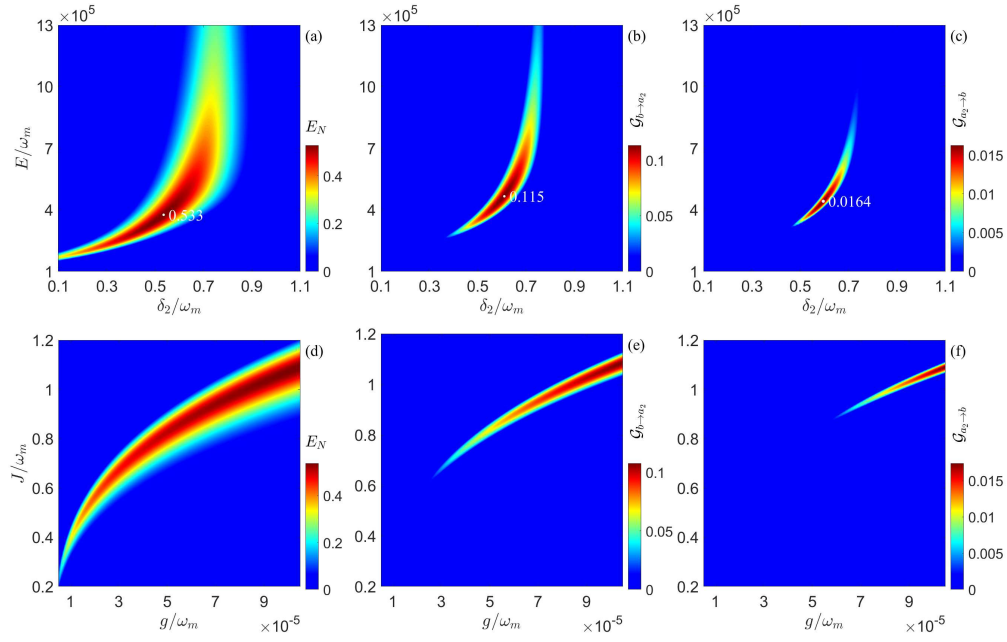


Fig. 4. The dynamics of entanglement E_N (a), steering $\mathcal{G}_{b \rightarrow a_2}$ (b), and $\mathcal{G}_{a_2 \rightarrow b}$ (c) as functions of the detuning δ_2 and driving amplitude E . The variation in the corresponding nonlocality as functions of the single-photon coupling g and resonators coupling J are shown in (e)-(f). The system parameters are chosen as those in Fig. 2.

versus the detuning parameter δ_2 and drive amplitude E in panels (a)-(c). For comparison, the behaviour of entanglement and steering as functions of the single-photon coupling strength g and coupling strength J between the resonators are shown in panels (d)-(f). In all panels, the squeezing parameter is set as $r = 1$, and the corresponding strength of the pumping laser is $\Omega_p/\omega_m = 0.5$ with power $P_p = \frac{1}{16}\Omega_p^2\kappa_p\omega_p/\chi^2 \approx 1.1\text{nW}$ under detuning $\delta_2/\omega_m = 0.52$, $\delta/\omega_m = 0.5$ as an example [48]. The other parameters are the same as those in Fig. 2, and the Routh-Hurwitz criterion is applied throughout the article to ensure the system is in the stable regime [67].

In Figs. 4(a)-(c), strong steady-state entanglement and steering can be obtained in a broad regime by controlling the detuning δ_2 between the pumping laser and resonator a_2 and amplitude E of the driving laser of the resonator a_1 . However, a stronger amplitude is not always better, and the maximum values, i.e., $E_N \approx 0.533$, $\mathcal{G}_{b \rightarrow a_2} \approx 0.115$, and $\mathcal{G}_{a_2 \rightarrow b} \approx 0.0164$, are marked. In Hamiltonian (10), the effective detuning Δ_2 is related to the squeezing parameter r and grows with the detuning δ_2 homologically. In contrast, the effective coupling strength G will be enhanced by increasing both Δ_2 and E and is majorly influenced by the driving amplitude E due to the magnitude difference. With increasing G , the squeezing coefficient λ in the Bogoliubov mode β will decrease monotonically, and the entanglement will reduce seemingly. However, based on the physical mechanism analysis, increasing G will strengthen the effective interaction η between the resonator mode δa_1 and Bogoliubov mode β , which will lead to a stronger cooling effect on the Bogoliubov mode β . The result of the competitive and cooperative effects between these two opposite effects on entanglement is shown in panel (a). In essence, both EPR steering and quantum entanglement stem from the nonlocality of quantum mechanics. However, EPR steering is stronger than quantum entanglement under the hierarchy of quantum nonlocality, so the nonzero steering regions are smaller than those of quantum entanglement. Moreover, due

to the intrinsic asymmetrical feature of EPR steering, one can also investigate one-way and two-way steering between modes δa_2 and δb (see Fig. 5 below).

In panels (d)-(f), we show the variation in the quantum entanglement and EPR steering along with the single-photon coupling strength g and resonator coupling strength J . The effective optomechanical coupling strength G will be enhanced with increasing g , and the coefficients λ and η of the Bogoliubov mode β will be enhanced synchronously. Based on the mechanism of entanglement generation, a larger λ will lead to stronger entanglement. Moreover, a larger η will reinforce the cooling effect on the Bogoliubov mode β , which will further strengthen the entanglement, as shown in panel (d), where the maximum value of entanglement increases monotonically with g . However, the entanglement cannot be increased indefinitely with increasing g . On the one hand, $\cosh \lambda$ and $\sinh \lambda$ will asymptotically equal with increasing λ , and the maximal entanglement will arrive asymptotically; on the other hand, the cooling effect on the Bogoliubov mode β is limited due to the employment of the RWA approximation. When the interaction strength η is strong enough, the counter rotating-wave term cannot be eliminated, and the corresponding Stokes effect will heat the Bogoliubov mode, which will counteract the cooling effect by the anti-Stokes effect and limit the maximal steady-state entanglement. In addition, it isn't easy to experimentally achieve a very strong single-photon coupled optomechanical system. A larger value of J will decrease G and η and increase λ , which will lead to maximal

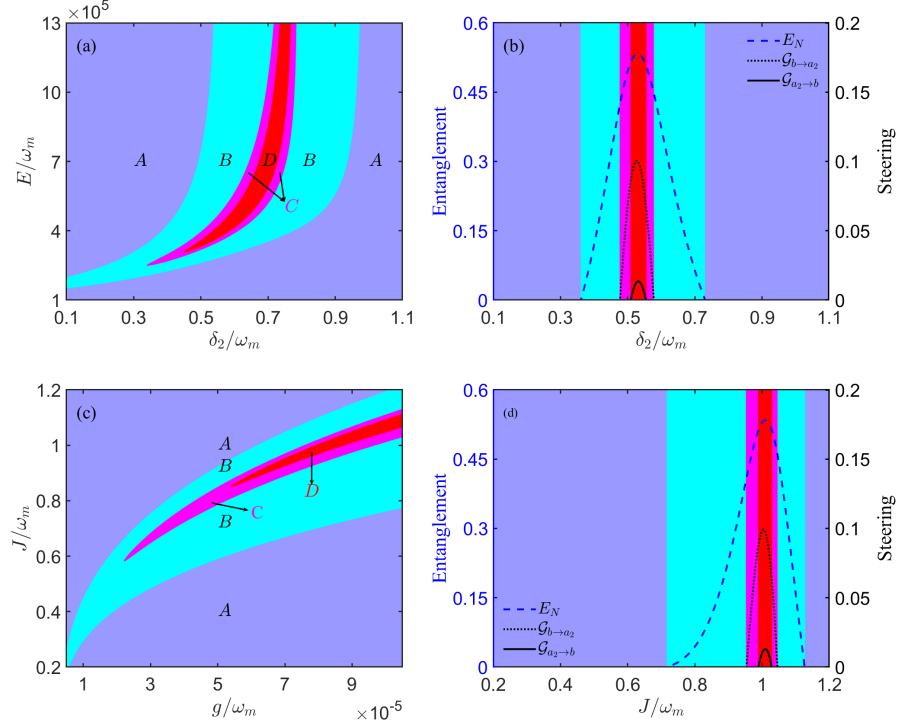


Fig. 5. The regimes of zero/nonzero entanglement, one-way steering and two-way steering. The lilac regimes are zero entanglement regions and marked by A; the cyan regimes are nonzero entanglement without steering regions and marked by B; the magenta regimes are one-way steering $\mathcal{G}_{b \rightarrow a_2}$ regions and marked by C; the red regimes are the two-way steering regions, and marked by D. In (b) and (d), the blue dashed line is the quantum entanglement; the black dotted line denotes the EPR steering $\mathcal{G}_{b \rightarrow a_2}$; and the black line shows the EPR steering $\mathcal{G}_{a_2 \rightarrow b}$.

entanglement for a modest value of J due to the competition between λ and η . The dynamics of EPR steering have a very similar physical mechanism, and its nonzero regions have distinct differences from quantum entanglement, which will be investigated in the following.

In Fig. 5, we plot regimes where the system has nonzero entanglement, one-way and two-way steering. The system parameters are chosen as those of maximal quantum entanglement in Fig. 4. The lilac regimes denote that there does not exist quantum entanglement, which are marked by regions *A* in panels (a) and (c); the cyan regimes denote that there exists nonzero quantum entanglement, while the EPR steering is absent, which are marked by regions *B*; the magenta regimes (marked by regions *C*) denote that there only exists one-way steering $\mathcal{G}_{b \rightarrow a_2}$, i.e., the mechanical mode δb can steer the resonator mode δa_2 , while the resonator mode δa_2 cannot steer the mechanical mode δb ; the red regimes, i.e., marked by regions *D*, present that there exists two-way steering, and both the modes δa_2 and δb can steer each other. As a vivid exhibition, we plot the variation in quantum entanglement and EPR steering versus the detuning δ_2 between the resonator a_2 and pumping laser in panel (b). The left axis denotes the quantum entanglement, which is expressed by the blue dashed line, while the EPR steering is described by the right axis with the black dotted line $\mathcal{G}_{b \rightarrow a_2}$ and the black line $\mathcal{G}_{a_2 \rightarrow b}$. The variation in quantum entanglement and EPR steering versus the coupling strength J is shown in panel (d), which can be realized by adjusting the gap between the resonators a_1 and a_2 . From panels (b) and (d), one can find the transition from zero entanglement to strong entanglement and one-way steering to two-way steering through modulating the detuning δ_2 or the coupling strength J , which is easy to implement experimentally.

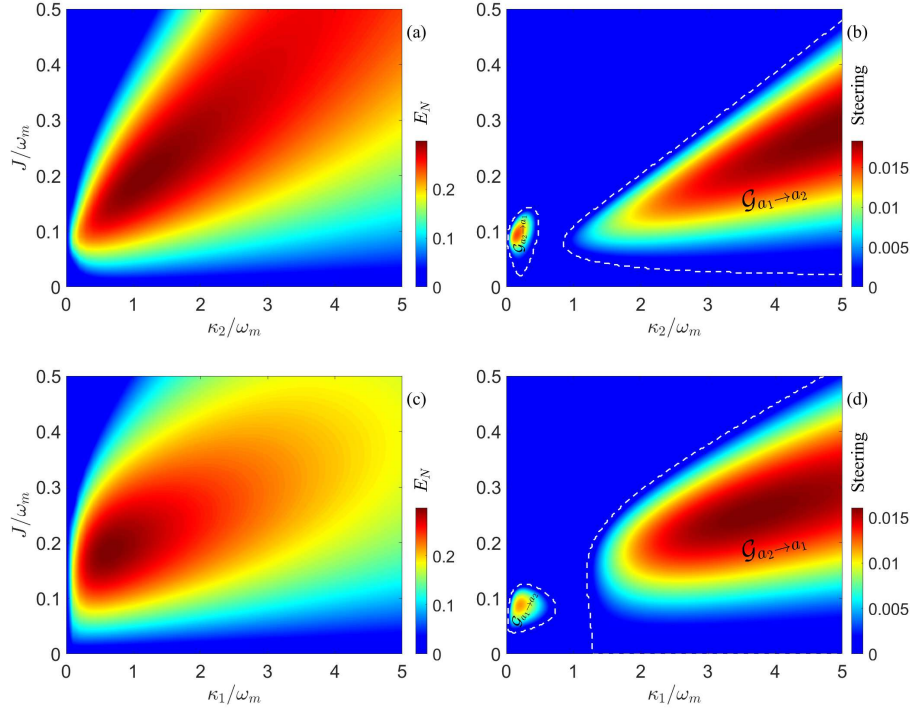


Fig. 6. The variation in quantum entanglement and EPR steering versus the coupling strength and resonator decay rate. The amplitude of the driving laser is $E/\omega_m = 0.5 \times 10^4$, the detuning of the resonator a_2 and pumping laser is $\delta_2/\omega_m = 0.8$, and the other parameters are the same as those in Fig. 4.

4. Entanglement and steering of resonators a_1 and a_2

In this section, we will investigate the quantum nonlocality between the two resonators a_1 and a_2 . In contrast to the quantum nonlocality of the resonator mode δa_2 and mechanical mode δb , there is no quantum entanglement when the amplitude E of the driving laser is strong. According to Hamiltonian (10), the mechanical mode δb can be cooled by the optical mode δa_1 due to the beam-splitter interaction $G(\delta a_1 \delta b^\dagger + \delta a_1^\dagger \delta b)$ under red-detuning driving, which will inhibit the quantum entanglement between resonators a_1 and a_2 . The strength of effective interaction G should be reduced to generate strong quantum entanglement. Due to $G = g a_{1s}$, there are two main approaches to decrease the value of G , i.e., weaken the driving amplitude E or strengthen the squeezing parameter r . If the system's stability is considered, the value of r should not be too large. When the red-detuning condition $\Delta'_1 = \omega_m$ is employed, the effective coupling strength G is mainly determined by the driving amplitude E , and the positive influence on the quantum entanglement can be realized by appropriately decreasing the value of E . In Fig. 6, we plot the quantum entanglement and EPR steering versus the coupling strength J and resonator decay rate κ_1 and κ_2 , respectively. Panels (a) and (c) show the quantum entanglement, and the variations in EPR steering are shown in panels (b) and (d). The detuning δ_2/ω between the pumping laser and resonator a_2 is tuned to 0.8, the driving amplitude is $E/\omega = 0.5 \times 10^4$, and the other parameters are the same as those given in Fig. 3. One can find that the maximal quantum entanglement occurs in the vicinity of $\kappa_1 \approx \kappa_2$ and always in the regime in which κ_2 is slightly larger than κ_1 . Intuitively, the quantum entanglement between two modes is symmetric, and the maximal quantum entanglement should occur where the two resonators have the same properties. It can be considered an additional decay path for the resonator a_1 with optomechanical interaction, such as $g/\omega_m = 8.5 \times 10^{-5}$, so there needs to be a greater decay rate κ_2 to balance the “additional decay rate” of κ_1 , which are shown in panels (a) and (c). Due to the direct interaction between the two resonators, the coupling strength J should not be too large to exchange photons, which is in contrast to the optomechanical entanglement behavior in Fig. 4. Another striking feature of the entanglement between resonators a_1 and a_2 is the one-way EPR steering. The variation in EPR steering with decay rate κ_2 is shown in Fig. 6(b). The nonzero steering $\mathcal{G}_{a_2 \rightarrow a_1}$ regime is in the lower left region, which means that mode δa_2 can steer mode δa_1 ; while the nonzero steering $\mathcal{G}_{a_1 \rightarrow a_2}$ regime is in the right region, which denotes that mode δa_1 can steer mode δa_2 . In the stable regime, there does not exist two-way EPR steering, which is markedly different from the steering between the resonator a_2 and mechanical oscillator b . By controlling the decay rate, we can manipulate and utilize unidirectional EPR steering to implement a desired quantum process. Similarly, the EPR steering versus the decay rate κ_1 is shown in panel (d).

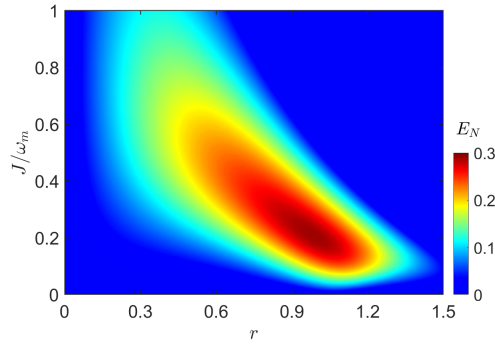


Fig. 7. The variation in quantum entanglement along with the coupling strength and squeezing parameter. The system parameters are the same as those in Fig. 6.

The quantum entanglement between resonators a_1 and a_2 versus the coupling strength J and squeezing parameter r are shown in Fig. 7. One can find that the coupling between resonators a_1 and a_2 and the squeezing of resonator a_2 induced by the pumping laser is necessary to generate quantum entanglement. Even though the squeezing parameter r can strengthen the effective coupling strength J^s between the modes δa_1 and δa_2 , the large J^s harms entanglement, which is similar to the analysis in Fig. 6. The strength of the original coupling J should also be moderate, and there is a similar detrimental effect to entanglement with large J . Therefore, the key to generating strong entanglement is optimizing the squeezing parameter r based on the system parameters rather than simply raising the value of r .

5. Conclusions

Quantum entanglement and EPR steering are important characteristics that distinguish quantum systems from the classical world and significant physical resources in modern quantum technology, and how to generate quantum entanglement and EPR steering is at the heart of related research. This paper proposes a theoretical proposal to manipulate optomechanical entanglement and EPR steering induced by quantum squeezing in a coupled WGM optomechanical system. By pumping the $\chi^{(2)}$ -nonlinear resonator with a phase matching condition, strong entanglement and steering between the mechanical oscillator and the indirect interacted squeezed resonator can be generated, where the squeezing of the $\chi^{(2)}$ -nonlinear resonator plays a vital role in this process. By adjusting the system parameters, such as the detuning of the pumping $\chi^{(2)}$ -nonlinear resonator or the coupling strength between the two resonators, the transitions from zero entanglement to strong entanglement and one-way steering to two-way steering can be realized in the stable regime. Meanwhile, the photon-photon entanglement of the coupled resonators can be obtained by weakening the driving laser's amplitude, and nonreciprocal one-way steering can be realized by changing the decay rates. This project paves a flexible, convenient, and innovative avenue to utilize optomechanical or photon-photon entanglement in quantum technology since there is no extraordinary squeezed field in this project, and entanglement and steering can be realized by controlling the system parameters. Because multi-body entanglement has richer properties than two-body entanglement and may have greater advantages in quantum processes, the multi-body entanglement among the three modes in this project and the role of squeezing in it are worthy of systematic investigation in the following works.

Funding. National Key Research and Development Program of China (2021YFA1402002), National Natural Science Foundation of China (U21A20433, 12175029, and 12204440), Fundamental Research Program of Shanxi Province (20210302123063, and 202103021223184).

Disclosures. The authors declare no conflicts of interest.

Data Availability. The data that support the findings of this study are available upon reasonable request from the authors.

References

1. M. Aspelmeyer, T. J. Kippenberg, and F. Marquardt, "Cavity optomechanics," *Rev. Mod. Phys.* **86**(4), 1391-1452 (2014).
2. D. Vitali, S. Gigan, A. Ferreira, H. R. Böhm, P. Tombesi, A. Guerreiro, V. Vedral, A. Zeilinger, and M. Aspelmeyer, "Optomechanical entanglement between a movable mirror and a cavity field," *Phys. Rev. Lett.* **98**(3), 030405 (2007).
3. M. Paternostro, D. Vitali, S. Gigan, M. S. Kim, C. Brukner, J. Eisert, and M. Aspelmeyer, "Creating and probing multipartite macroscopic entanglement with light," *Phys. Rev. Lett.* **99**(25), 250401 (2007).
4. D. G. Lai, W. Qin, B. P. Hou, A. Miranowicz, and F. Nori, "Significant enhancement in refrigeration and entanglement in auxiliary-cavity-assisted optomechanical systems," *Phys. Rev. A* **104**(4), 043521 (2021).
5. A. Mari and J. Eisert, "Gently modulating optomechanical systems," *Phys. Rev. Lett.* **103**(21), 213603 (2009).
6. M. Wang, X. Y. Lü, Y. D. Wang, J. Q. You, and Y. Wu, "Macroscopic quantum entanglement in modulated optomechanics," *Phys. Rev. A* **94**(5), 053807 (2016).

7. D. Miki, N. Matsumoto, A. Matsumura, T. Shichijo, Y. Sugiyama, K. Yamamoto, and N. Yamamoto, "Generating quantum entanglement between macroscopic objects with continuous measurement and feedback control," *Phys. Rev. A* **107**(3), 032410 (2023).
8. Y. F. Jiao, S. D. Zhang, Y. L. Zhang, A. Miranowicz, L. M. Kuang, and H. Jing, "Nonreciprocal optomechanical entanglement against backscattering losses," *Phys. Rev. Lett.* **125**(14), 143605 (2020).
9. D. G. Lai, J. Q. Liao, A. Miranowicz, and F. Nori, "Noise-tolerant optomechanical entanglement via synthetic magnetism," *Phys. Rev. Lett.* **129**(6), 063602 (2022).
10. Z. Q. Liu, C. S. Hu, Y. K. Jiang, W. J. Su, H. Wu, Y. Li, and S. B. Zheng, "Engineering optomechanical entanglement via dual-mode cooling with a single reservoir," *Phys. Rev. A* **103**(2), 023525 (2021).
11. X. Hu, "Entanglement generation by dissipation in or beyond dark resonances," *Phys. Rev. A* **92**(2), 022329 (2015).
12. C. S. Hu, Z. Q. Liu, Y. Liu, L. T. Shen, H. Wu, and S. B. Zheng, "Entanglement beating in a cavity optomechanical system under two-field driving," *Phys. Rev. A* **101**(3), 033810 (2020).
13. C. F. Ockeloen-Korppi, E. Damskäg, J. M. Pirkkalainen, M. Asjad, A. A. Clerk, F. Massel, M. J. Woolley, and M. A. Sillanpää, "Stabilized entanglement of massive mechanical oscillators," *Nature* **556**, 478-482 (2018).
14. C. Genes, D. Vitali, and P. Tombesi, "Emergence of atom-light-mirror entanglement inside an optical cavity," *Phys. Rev. A* **77**(5), 050307(R) (2008).
15. J. Li, S. Y. Zhu, and G. S. Agarwal, "Magnon-photon-phonon entanglement in cavity magnomechanics," *Phys. Rev. Lett.* **121**(20), 203601 (2018).
16. X. Z. Hao, X. Y. Zhang, Y. H. Zhou, W. Li, S. C. Hou, and X. X. Yi, "Dynamical bipartite and tripartite entanglement of mechanical oscillators in an optomechanical array," *Phys. Rev. A* **104**(5), 053515 (2021).
17. A. Einstein, B. Podolsky, and N. Rosen, "Can quantum-mechanical description of physical reality be considered complete?" *Phys. Rev.* **47**(10), 777-780 (1935).
18. E. Schrödinger, "Discussion of probability relations between separated systems," *Math. Proc. Cambridge Philos. Soc.* **31**, 555-563 (1935).
19. R. Uola, A. C. S. Costa, H. C. Nguyen, and O. Gühne, "Quantum steering," *Rev. Mod. Phys.* **92**(1), 015001 (2020).
20. M. D. Reid, P. D. Drummond, W. P. Bowen, E. G. Cavalcanti, P. K. Lam, H. A. Bachor, U. L. Andersen, and G. Leuchs, "Colloquium: The Einstein-Podolsky-Rosen paradox: from concepts to applications," *Rev. Mod. Phys.* **81**(4), 1727-1751 (2009).
21. I. Kogias, A. R. Lee, S. Ragy, and G. Adesso, "Quantification of Gaussian quantum steering," *Phys. Rev. Lett.* **114**(6), 060403 (2015).
22. Q. He, L. Rosales-Zárate, G. Adesso, and M. D. Reid, "Secure continuous variable teleportation and Einstein-Podolsky-Rosen steering," *Phys. Rev. Lett.* **115**(18), 180502 (2015).
23. M. Frigerio, S. Olivares, and M. G. A. Paris, "Steering nonclassicality of Gaussian states," *Phys. Rev. A* **103**(2), 022209 (2021).
24. R. Y. Teh, M. Gessner, M. D. Reid, and M. Fadel, "Full multipartite steering inseparability, genuine multipartite steering, and monogamy for continuous-variable systems," *Phys. Rev. A* **105**(1), 012202 (2022).
25. R. V. Nery, M. M. Taddei, P. Sahium, S. P. Walborn, L. Aolita, and G. H. Aguilar, "Distillation of quantum steering," *Phys. Rev. Lett.* **124**(12), 120402 (2020).
26. X. Deng, Y. Xiang, C. Tian, G. Adesso, Q. He, Q. Gong, X. Su, C. Xie, and K. Peng, "Demonstration of monogamy relations for Einstein-Podolsky-Rosen steering in Gaussian cluster states," *Phys. Rev. Lett.* **118**(23), 230501 (2017).
27. L. Ma, X. Lei, J. Cheng, Z. Yan, and X. Jia, "Deterministic manipulation of steering between distant quantum network nodes," *Opt. Express* **31**(5), 8257-8266 (2023).
28. Y. Liang, R. Yang, J. Zhang, and T. Zhang, "Hexapartite steering based on a four-wave-mixing process with a spatially structured pump," *Opt. Express* **31**(7), 11775-11787 (2023).
29. D. Kong, J. Xu, Y. Tian, F. Wang, and X. Hu, "Remote asymmetric Einstein-Podolsky-Rosen steering of magnons via a single pathway of Bogoliubov dissipation," *Phys. Rev. Res.* **4**(1), 013084 (2022).
30. Q. Guo, M. R. Wei, C. H. Bai, Y. Zhang, G. Li, and T. Zhang, "Manipulation and enhancement of Einstein-Podolsky-Rosen steering between two mechanical modes generated by two Bogoliubov dissipation pathways," *Phys. Rev. Res.* **5**(1), 013073 (2023).
31. S. Zheng, F. Sun, Y. Lai, Q. Gong, and Q. He, "Manipulation and enhancement of asymmetric steering via interference effects induced by closed-loop coupling," *Phys. Rev. A* **99**(2), 022335 (2019).
32. H. Tan and J. Li, "Einstein-Podolsky-Rosen entanglement and asymmetric steering between distant macroscopic mechanical and magnonic systems," *Phys. Rev. Res.* **3**(1), 013192 (2021).
33. Y. C. Liu, Y. F. Xiao, X. Luan, Q. Gong, and C. W. Wong, "Coupled cavities for motional ground-state cooling and strong optomechanical coupling," *Phys. Rev. A* **91**(3), 033818 (2015).
34. C. H. Bai, D. Y. Wang, S. Zhang, S. Liu, and H. F. Wang, "Engineering of strong mechanical squeezing via the joint effect between Duffing nonlinearity and parametric pump driving," *Photon. Res.* **7**(11), 1229-1239 (2019).
35. J. Q. Liao and C. K. Law, "Parametric generation of quadrature squeezing of mirrors in cavity optomechanics," *Phys. Rev. A* **83**(3), 033820 (2011).
36. R. Zhang, Y. Fang, Y. Y. Wang, S. Chesi, and Y. D. Wang, "Strong mechanical squeezing in an unresolved-sideband optomechanical system," *Phys. Rev. A* **99**(4), 043805 (2019).
37. C. W. Wang, W. Niu, Y. Zhang, J. Cheng, and W. Z. Zhang, "Optomechanical noise suppression with the optimal squeezing process," *Opt. Express* **31**(7), 11561-11577 (2023).

38. B. Xiong, S. Chao, C. Shan, and J. Liu, "Optomechanical squeezing with pulse modulation," *Opt. Lett.* **47**(21), 5545-5548 (2022).
39. J. Huang, D. G. Lai, C. Liu, J. F. Huang, F. Nori, and J. Q. Liao, "Multimode optomechanical cooling via general dark-mode control," *Phys. Rev. A* **106**(1), 013526 (2022).
40. G. S. Agarwal and S. Huang, "Strong mechanical squeezing and its detection," *Phys. Rev. A* **93**(4), 043844 (2016).
41. W. Zhang, T. Wang, X. Han, S. Zhang, and H. F. Wang, "Mechanical squeezing induced by Duffing nonlinearity and two driving tones in an optomechanical system," *Phys. Lett. A* **424**, 127824(2022).
42. P. Vezio, A. Chowdhury, M. Bonaldi, A. Borrielli, F. Marino, B. Morana, G.A. Prodi, P.M. Sarro, E. Serra, and F. Marin, "Quantum motion of a squeezed mechanical oscillator attained via an optomechanical experiment," *Phys. Rev. A* **102**(5), 053505 (2020).
43. J. Yang, C. Zhao, Z. Yang, R. Peng, S. Chao, and L. Zhou, "Nonreciprocal ground-state cooling of mechanical resonator in a spinning optomechanical system," *Front. Phys.* **17**, 52507 (2022).
44. X. Y. Lü, Y. Wu, J. R. Johansson, H. Jing, J. Zhang, and F. Nori, "Squeezed optomechanics with phase-matched amplification and dissipation," *Phys. Rev. Lett.* **114**(9), 093602 (2015).
45. W. Qin, A. Miranowicz, P. B. Li, X. Y. Lü, J. Q. You, and F. Nori, "Exponentially enhanced light-matter interaction, cooperativities, and steady-state entanglement using parametric amplification," *Phys. Rev. Lett.* **120**(9), 093601 (2018).
46. Y. Wang, C. Li, E. M. Sampuli, J. Song, Y. Jiang, and Y. Xia "Enhancement of coherent dipole coupling between two atoms via squeezing a cavity mode," *Phys. Rev. A* **99**(2), 023833 (2019).
47. Y. J. Ma, X. C. Gao, S. X. Wu, and C. S. Yu, "Quantum speed limit of a single atom in a squeezed optical cavity mode," *Chin. Phys. B* **32**(4), 040308 (2023).
48. L. Tang, J. Tang, M. Chen, F. Nori, M. Xiao, and K. Xia, "Quantum squeezing induced optical nonreciprocity," *Phys. Rev. Lett.* **128**(8), 083604 (2022).
49. B. Peng, S. K. Özdemir, F. Lei, F. Monifi, M. Gianfreda, G. L. Long, S. Fan, F. Nori, C. M. Bender, and L. Yang, "Parity-time-symmetric whispering-gallery microcavities," *Nature Phys.* **10**, 394-398 (2014).
50. L. Chang, X. Jiang, S. Hua, C. Yang, J. Wen, L. Jiang, G. Li, G. Wang, and M. Xiao, "Parity-time symmetry and variable optical isolation in active-passive-coupled microresonators," *Nature Photon.* **8**, 524-529 (2014).
51. H. Jing, Ş. K. Özdemir, Z. Geng, J. Zhang, X. Y. Lü, B. Peng, L. Yang, and F. Nori, "Optomechanically-induced transparency in parity-time-symmetric microresonators," *Sci. Rep.* **5**, 9663 (2015).
52. Z. Shen, Y. L. Zhang, Y. Chen, Y. F. Xiao, C. L. Zou, G. C. Guo, and C. H. Dong, "Nonreciprocal frequency conversion and mode routing in a microresonator," *Phys. Rev. Lett.* **130**(1), 013601 (2023).
53. C. Lei and J. Ren, "Quantum-interference-enhanced phonon laser in cavity optomechanics," *Phys. Rev. Appl.* **19**(5), 054093 (2023).
54. D. Y. Wang, L. L. Yan, S. L. Su, C. H. Bai, H. F. Wang, and E. Liang, "Squeezing-induced nonreciprocal photon blockade in an optomechanical microresonator," *Opt. Express* **31**(14), 22343-22357 (2023).
55. Z. Li, X. Li, and X. Zhong, "Optomechanical entanglement affected by exceptional point in a WGM resonator system," *Opt. Express* **31**(12), 19382-19391 (2023).
56. W. Zhang, T. Wang, X. Han, S. Zhang, and H. F. Wang, "Quantum entanglement and one-way steering in a cavity magnomechanical system via a squeezed vacuum field," *Opt. Express* **30**(7), 10969-10980 (2022).
57. S. X. Wu, C. H. Bai, G. Li, C. S. Yu, and T. Zhang, "Enhancing the quantum entanglement and EPR steering of a coupled optomechanical system with a squeezed vacuum field," *J. Opt. Soc. Am. B* **40**(11), 2885-2893 (2023).
58. Y. D. Wang and A. A. Clerk, "Reservoir-engineered entanglement in optomechanical systems," *Phys. Rev. Lett.* **110**(25), 253601 (2013).
59. J. Li, I. M. Haghghi, N. Malossi, S. Zippilli, and D. Vitali, "Generation and detection of large and robust entanglement between two different mechanical resonators in cavity optomechanics," *New J. Phys.* **17**(10) 103037 (2015).
60. C. W. Gardiner and P. Zoller, *Quantum noise*, 2nd ed. (Berlin, Springer, 2000).
61. M. O. Scully and M. S. Zubairy, *Quantum optics*. (Cambridge, Cambridge University Press, 1997).
62. G. Vidal and R. F. Werner, "Computable measure of entanglement," *Phys. Rev. A* **65**(3), 032314 (2002).
63. G. Adesso, A. Serafini, and F. Illuminati, "Extremal entanglement and mixedness in continuous variable systems," *Phys. Rev. A* **70**(2), 022318 (2004).
64. M. B. Plenio, "Logarithmic Negativity: A full entanglement monotone that is not convex," *Phys. Rev. Lett.* **95**, 090503 (2005).
65. L. M. Duan, G. Giedke, J. I. Cirac, and P. Zoller, "Inseparability criterion for continuous variable systems," *Phys. Rev. Lett.* **84**(12), 2722-2725 (2000).
66. R. Simon, "Peres-Horodecki separability criterion for continuous variable systems," *Phys. Rev. Lett.* **84**(12), 2726-2729 (2000).
67. E. X. DeJesus and C. Kaufman, "Routh-Hurwitz criterion in the examination of eigenvalues of a system of nonlinear ordinary differential equations," *Phys. Rev. A* **35**(12), 5288-5290 (1987).